Crystallization and Melting Behavior of Poly(ferrocenyldimethylsilanes) Obtained by Anionic Polymerization

Rob G. H. Lammertink,‡ Mark A. Hempenius,‡ Ian Manners,† and G. Julius Vancso*,‡

Faculty of Chemical Technology, University of Twente, P.O. Box 217, NL-7500 AE Enschede, The Netherlands, and Department of Chemistry, University of Toronto, 80 St. George Street, Toronto, Ontario M5S 3H6, Canada

Received July 25, 1997; Revised Manuscript Received December 1, 1997

ABSTRACT: A series of poly(ferrocenyldimethylsilanes) (PFS) with narrow molar mass distribution were prepared via anionic ring-opening polymerization. The thermal behavior and morphology of these materials were investigated. Differential scanning calorimetry (DSC) experiments showed multiple melting endotherms upon heating after isothermal crystallization. Melting of thin lamellae and recrystallization into thicker lamellae accounted for these multiple transitions. Wide-angle X-ray scattering (WAXS) showed that the crystal structure remained unchanged during heating. An increase in the long-period observed with temperature-dependent small-angle X-ray scattering (SAXS) supported the assumption that lamellar thickening occurs. The semicrystalline polymers showed a melting behavior as described by the Hoffman−Weeks equation, leading to an equilibrium melting temperature of 143 °C.

Introduction

Polymers which contain inorganic elements or organometallic units in the main chain are of considerable interest as a result of their novel electrical, optical, magnetic, and chemical characteristics.[1,2] Poly(ferrocenylsilanes), consisting of alternating ferrocenyl units and silicon atoms in the main chain, are part of this class of potentially useful macromolecules.

Since the 1970s, poly(ferrocenylsilanes) were made accessible via a condensation polymerization of dilithioferrocene and dichlorodialkylsilane.[3] However, the recent discovery of the ring-opening polymerization (ROP) of silicon bridged ferrocenophane[4] has increased the opportunities for the tailoring of poly(ferrocenylsilanes). For example, thermal ROP[4] and γ−irradiation[5] in the solid state produces high molar mass poly(ferrocenylsilanes). Transition-metal catalyzed[6] ROP allows the synthesis of regioregular poly(ferrocenylsilanes). Anionic polymerization leads to poly(ferrocenylsilanes) with controlled molar masses and low polydispersities.[7] Using these methods, a range of novel polymers have been synthesized, featuring the following variations: substituents on silicon,[8,9] number and type of bridging atoms,[10] and substituents on the cyclopentadienyl rings.[11]

The electrochemical properties of these novel organometallic materials have been studied in some detail.[8,12] Poly(ferrocenylsilanes) possess electrochemical characteristics indicating intermetallic electronic coupling between the iron atoms.[13] The understanding and control of effective Fe−Fe interactions is relevant for potentially important bulk magnetic properties. Furthermore, poly(ferrocenylsilanes) can serve as pyrolytic precursors to magnetic iron silicon carbide ceramics.[14]

So far, no systematic investigation on the thermal behavior of poly(ferrocenylsilanes) has been reported in the literature. Knowledge on the crystallization and melting behavior of these novel polymers is of interest, and furthermore, it supports the further exploration of their electronic and magnetic properties. This paper describes the thermal behavior and morphology of a series of well-defined poly(ferrocenyldimethylsilanes), prepared via anionic ring-opening polymerization.

Experimental Section

N,*N*,*N*′,*N*′-Tetramethylethylenediamine (TMEDA), ferrocene, dichlorodimethylsilane, and *n*-butyllithium were purchased from Aldrich. TMEDA was distilled from sodium, and ferrocene was Soxhlet extracted with cyclohexane prior to use. Dimethylsilylferrocenophane was prepared as described earlier.[15,16] Polymerization was carried out in THF in a glovebox purged with prepurified nitrogen. *n*-Butyllithium was used as initiator, and the reaction was terminated after 2 h by adding a few drops of methanol. The polymers were precipitated twice in methanol and dried in vacuo.

GPC measurements were carried out in THF using microstyragel columns with pore sizes of 10^5, 10^4, 10^3, and 10^6 Å (Waters) equipped with a dual detection system consisting of a differential refractometer (Waters model 410) and a differential viscometer (Viscotek model H502). The molar masses were referenced to a polystyrene calibration curve. A Perkin-Elmer DSC-7 equipped with a PE−7700 computer using TAS-7 software was used for thermal analysis. In DSC experiments, unless otherwise reported, a scan rate of 10 K/min was employed. T_g values quoted in this study correspond to the inflection point at the heat capacity change as determined by the software of the equipment used. Melting temperatures were taken from the peak maximum. Isothermal crystallizations experiments were performed by quenching (300 K/min) the samples from the melt to a selected holding temperature. When crystallization was complete, the thermograms were recorded starting from the holding temperature.

Wide-angle X-ray scattering (WAXS) patterns were recorded by a Siemens D500 diffractometer equipped with a water cooled hot stage. A Cu Kα X-ray source (λ = 1.542 Å) was used. The samples were melted on an aluminum plate, isothermally crystallized, and examined in reflection mode. The angle of diffraction, 2θ, ranged from 5 to 30°. A step size of 0.1° with a collection time of 12 s for each step was used. Small-angle X-ray scattering (SAXS) experiments were performed using a Kratky camera (Paar, Graz) in vacuo and a

* Corresponding author.
† University of Toronto.
‡ University of Twente.

S0024-9297(97)01124-8 CCC: $15.00
Published on Web 01/22/1998

Scheme 1

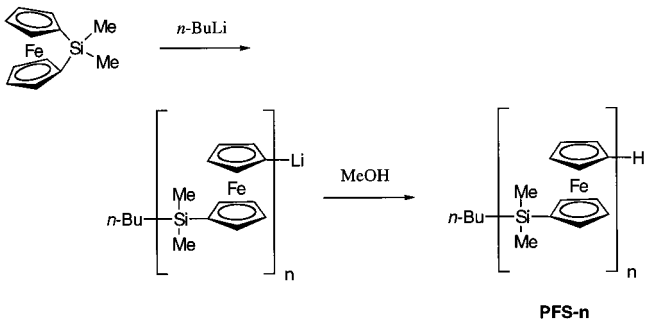

Table 1. Characteristics of the Poly(ferrocenyldimethylsilanes)[a]

	$\bar{M}_n$	$\bar{M}_w$	$\bar{M}_w/\bar{M}_n$
PFS-25	6500, 5800[b]	7100	1.09
PFS-50	11 400	12 500	1.09
PFS-100	24 200	26 200	1.09
PFS-200	44 900	49 500	1.10
PFS-350	76 700	87 100	1.14

[a] GPC in THF using polystyrene calibration curves. [b] Determined by end group analysis using ^{1}H-NMR.[17]

Cu Kα source (λ = 1.542 Å). A water-cooled hot stage controlled temperatures up to 300 °C with an accuracy of 0.4 °C. Thin samples of about 150 μm were pressed under 3 kN at 50 °C and slowly heated under vacuum inside the SAXS camera. From the melt the sample was cooled to the desired crystallization temperature, and the SAXS experiments were started. Measurements were performed at temperatures ranging from 90 to 160 °C. Atomic force microscopy (AFM) images were taken in air using a NanoScope III (Digital Instruments) equipped with a J scanner. The scans were carried out in contact mode utilizing a NanoProbe 100 μm triangular Si_3N_4 cantilever with a spring constant of 0.38 Nm^{-1}.

Results and Discussion

Anionic Ring-Opening Polymerizations. Polymerizations of 1,1′-dimethylsilylferrocenophane were carried out in THF using *n*-butyllithium as the initiator. The living polymerization was terminated by the addition of a few drops of methanol (Scheme 1). The polymers were precipitated in methanol and dried under vacuum.

The GPC traces showed narrow monomodal molar mass distributions. The molar mass of the polymer with the lowest degree of polymerization was also estimated by end group analysis using ^{1}H NMR.[17] The characteristics of the polymers are shown in Table 1.

A reasonable agreement exists between the molar mass according to GPC and ^{1}H NMR for specimen PFS-25. Also, the molar masses estimated from the ratio of monomer to initiator agree within 10% from the values obtained by GPC.

Thermal Transitions. The glass transition temperatures (T_g), determined with DSC on quenched samples at 10 K/min, heat capacity values (ΔC_p) at T_g, and the melt enthalpies (ΔH_m) of the poly(ferrocenyldimethylsilanes) with different molar mass are given in Table 2.

Due to the excess free volume associated with the chain ends, the value of T_g depends on the number average molar mass $\bar{M}_n$. According to Flory[18] the value of T_g is proportional to $1/M_n$. For many polymer systems a better fit can be obtained using O'Driscoll's equation.[19]

Table 2. Thermal Data of the Poly(ferrocenyldimethylsilanes)[a]

	T_g (°C)	ΔC_p (J/gK)	ΔH_m (J/g)
PFS-25	22.4	0.15	14.7
PFS-50	25.7	0.16	14.2
PFS-100	28.0	0.16	12.6
PFS-200	31.0	0.18	10.0
PFS-350	31.3	0.17	7.7

[a] T_g and ΔC_p were obtained from quenched samples and ΔH_m was obtained from the crystallization exotherm during slow cooling (1 K/min) from the melt.

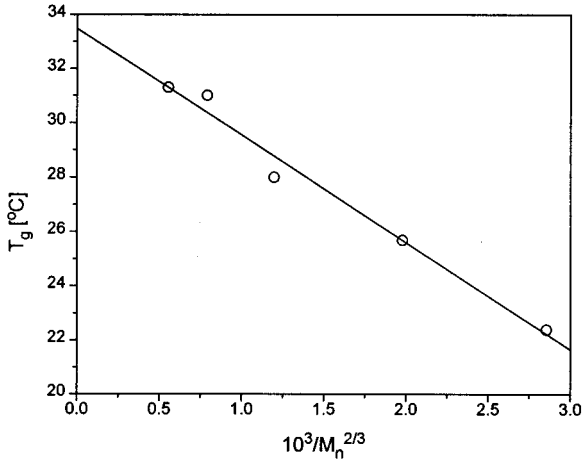

Figure 1. T_g as a function of $M_n^{-2/3}$ for poly(ferrocenyldimethylsilane).

According to O'Driscoll, the T_g can be described as

$$T_g = T_{g,\infty} - \frac{K}{M_n^{2/3}} \quad (1)$$

In this equation, $T_{g,\infty}$ is the glass transition temperature of the polymer with infinite molar mass, and the polymer-dependent constant K is related to the excess free volume at the chain ends. For poly(ferrocenyldimethylsilanes), the data shown in Tables 1 and 2 results in an extrapolated $T_{g,\infty}$ value of 33.5 °C. This value agrees well with the glass transition temperature of 33 °C observed for high molar mass poly(ferrocenyldimethylsilane), prepared via thermal ring-opening polymerization.[9] A fit of our data to eq 1 resulted in a regression coefficient of 0.991, as opposed to the regression coefficient of 0.981 for the $1/M_n$ fit (see Figure 1).

The values of the melting enthalpies ΔH_m, determined from the crystallization exotherm during slow cooling are given in Table 2. Cooling scans showed a single exotherm from which accurate ΔH_m values could be obtained. On the other hand, it was not possible to obtain meaningful ΔH_m values from heating scans as these displayed multiple endotherms. The magnitude of the melting enthalpies decreased with increasing molar masses.

Parts a−e of Figure 2 show the DSC heating traces for all polymers after isothermal crystallization at different temperatures. Before isothermal crystallization, the samples were kept in the melt for 5 min in order to erase any thermal history. After heating, the specimens were quenched (300 K/min) to the crystallization temperature indicated in Figure 2a−e. The crystallization process was monitored in time, and when completed, the corresponding heating trace was recorded starting directly from the crystallization temperature.

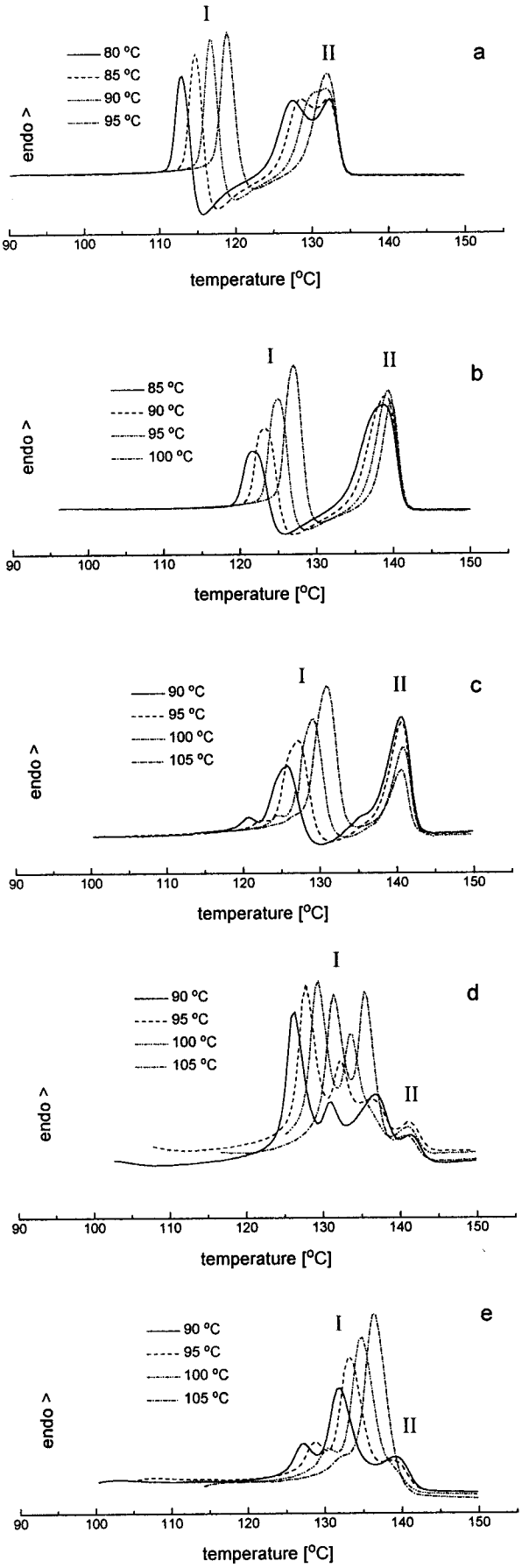

Figure 2. DSC scans (heat flow vs temperature) obtained at a scan rate of 10 K/min. Samples were crystallized isothermally at temperatures indicated on the figure: (a) PFS-25; (b) PFS-50; (c) PFS-100; (d) PFS-200; (e) PFS-350.

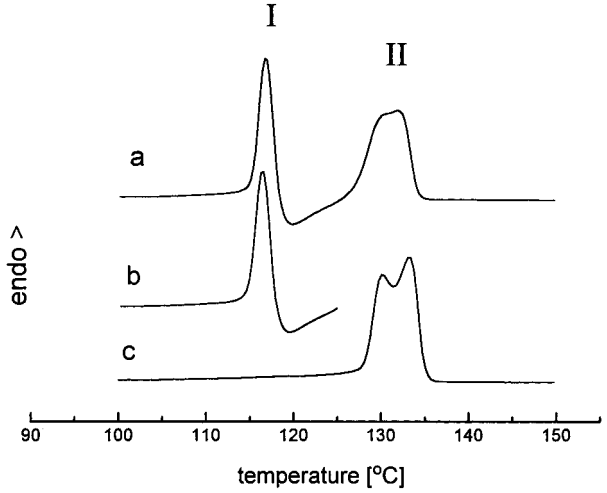

Figure 3. Irreversible melting illustrated for PFS-25: (a) melting after isothermal crystallization at 90 °C; (b) melting as in part a but scanned to 125 °C; (c) crystallization at 90 °C after scan b.

The heating scans display multiple melting transitions. Although such transitions are frequently observed in DSC experiments, their origins are not always well understood. Several models have been proposed in the literature. These include dual lamellar thickness models,[20,21] melting recrystallization models,[22,23] and physical aging models.[24]

In the heating traces of all polymers, two types of transitions indicated by I and II in the figures can be distinguished. The position of peak II is not affected by the isothermal crystallization temperature. In contrast, peaks of type I do depend on the crystallization temperature and shift to higher temperatures when a higher crystallization temperature was applied. A crystallization exotherm following transition I can be observed for samples PFS-25, PFS-50, and PFS-100 (see Figure 2a−c).

A striking feature on the DSC traces is that peak I is a result of an irreversible transition, as shown in Figure 3 for PFS-25. Scan a was taken up to 150 °C after the sample was crystallized at 90 °C. Scan b was recorded following the same thermal treatment, but was only obtained by scanning to a temperature of 125 °C. The sample was then cooled to 90 °C, allowing crystallization, and then reheated (scan c). Scan c shows that peak I completely disappeared due to the irreversible transition. Peak I can only be formed again after complete melting and crystallization.

From these results it can be concluded that a structural reorganization process occurs during the DSC scan. This was also confirmed by the observation that the enthalpy of peak II becomes smaller when higher scanning rates are applied, thus not allowing the sample to sufficiently reorganize. Similar reorganization processes are known for polymers such as PET,[25,26] PEEK,[27−30] and PE.[31] For these polymers it was found that peak I represents the melting point of the original crystals which are present prior to the first heating scan. Peak II was ascribed to the melting of reorganized crystals formed from the original crystals during heating.

The position of peak I (i.e. the temperature at which the reorganization occurs) depends on the crystallization temperature. For example, in Figure 2a, a sample of PFS-25 is crystallized at 80 °C, then partially melts and recrystallizes at approximately 112 °C (peak I). This

recrystallization temperature is still low enough to allow the formation of a structure which melts at a temperature lower than the final melting temperature (peak II), giving rise to an additional peak, visible as a shoulder, at the lower temperature side of peak II. If on the other hand, the sample is crystallized at 95 °C, recrystallization occurs at 120 °C (peak I), and the final melting transition occurs as a single peak II. At 120 °C, the supercooling is small enough to allow formation of the most stable structure.

The same dual melting behavior is observed for PFS-50 (Figure 2b) and PFS-100 (Figure 2c), but the transitions occur at slightly higher temperatures. (This may be due to the less pronounced diluting effect of the *n*-butyl end-groups). The shoulder in peak II is not visible, but the endotherm becomes broader at lower recrystallization temperatures. The higher molar mass polymer, PFS-200 (Figure 2d), displays an analogous behavior. Its DSC trace exhibits multiple transitions. The position of the lower temperature transitions depends on the crystallization temperature (type I) whereas a final melting endotherm remains at a constant temperature (type II). The members with lower molar mass, PFS-25, PFS-50, and PFS-100, display one melting transition followed by recrystallization. The higher polymer, PFS-200, showed additional melting endotherms. PFS-350 (Figure 2e) exhibits a melting behavior similar to PFS-200. Its type I transitions are crystallization temperature dependent as expected. The final peak II, only visible as a shoulder, is positioned at a constant temperature.

The position of peak I depends linearly on the crystallization temperature for all polymers. Its position may be influenced by the presence of the recrystallization exotherm.[32] It appears, however, the position of peak I is not affected to a great extent by the recrystallization exotherm since the enthalpy of peak I hardly changes when higher scanning rates are applied.

The position of peak I, T_m, can be described by the Hoffman−Weeks equation[33]

$$T_m = \frac{T_m^0(2\beta - 1) + T_c}{2\beta} \qquad (2)$$

in which T_m is the observed melting temperature, T_c the isothermal crystallization temperature, T_m^0 the extrapolated equilibrium melting temperature, and b the fold length in terms of primary, homogeneous nuclei. Figure 4 shows the Hoffman−Weeks plots for all polymers studied in this work using the position of the first peak I transition upon heating as T_m. This is because the transition belongs to the melting of the original crystals formed during the isothermal crystallization. The experimental data were fitted according to eq 2.

From the intersect $T_m = T_c = T_m^0$, the equilibrium melting temperature could be determined. For all polymers, except for PFS-25 (T_m^0 = 139 °C), an equilibrium melting temperature of 143 °C was found.

Previously, Manners et al.[34] reported on the melting points of oligomers of ferrocenyl dimethylsilanes having two to nine repeat units. These authors found that the melting point converged to 145 °C. This is in close agreement with the equilibrium melting temperature found for the polymers described here but is significantly higher than the previously reported melting temperature of 122 °C of high molar mass poly(ferrocenyldimethylsilane).[5,8]

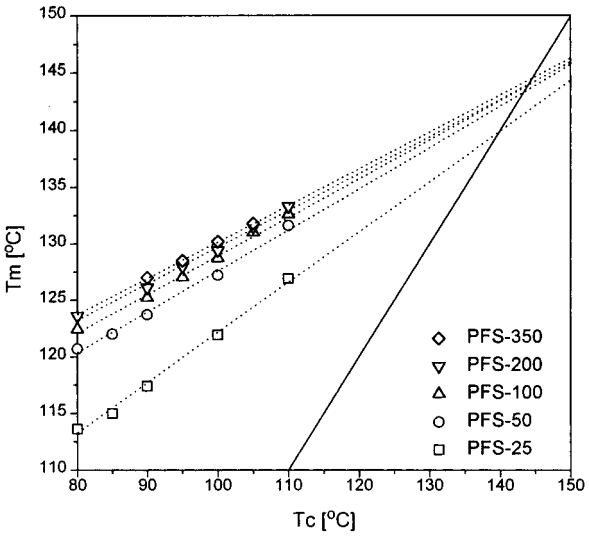

Figure 4. Hoffman−Weeks[33] plot of melting temperature vs crystallization temperature for poly(ferrocenyldimethylsilane) with different chain lengths.

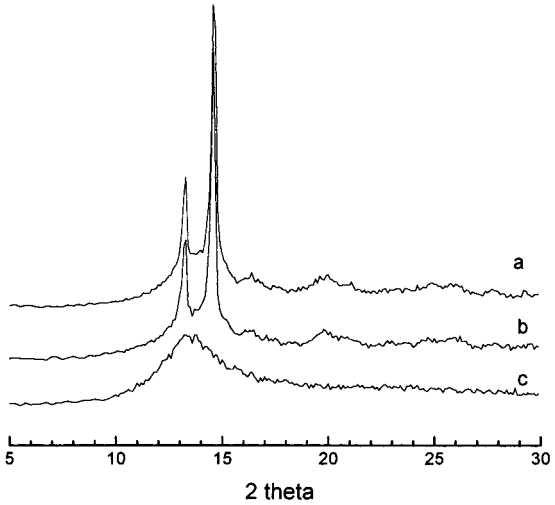

Figure 5. Wide-angle X-ray scattering intensity vs scattering angle for PFS-100 at (a) 100 °C, (b) 135 °C, and (c) 155 °C.

Morphology. Typical wide-angle X-ray scattering patterns for a melt-crystallized and amorphous poly(ferrocenyldimethylsilane) are shown in Figure 5 for PFS-100. The wide-angle X-ray pattern was obtained at 100, 135, and 155 °C (Figure 5a−c). The position of the main crystalline reflections at $2\theta = 13.3°$ and at $2\theta = 14.7°$ did not change with increasing temperature. This indicates that crystal structure transformations do not occur in this temperature region. The type I transition in the DSC experiments cannot therefore be ascribed to a crystal−crystal transformation.

Identical WAXS peak positions were observed for all polymers with different molar masses indicating that the crystal structure does not change with molar mass. The X-ray diffraction pattern for the semicrystalline PFS-100 (Figure 5a,b) exhibits two major peaks at distances of 6.65 and 6.02 Å. Previously, a wide-angle X-ray diffraction pattern was reported for high molar mass poly(ferrocenyldimethylsilane)[5,8] with one broad reflection positioned at 6.3 Å. The difference between this result and the patterns obtained in our work

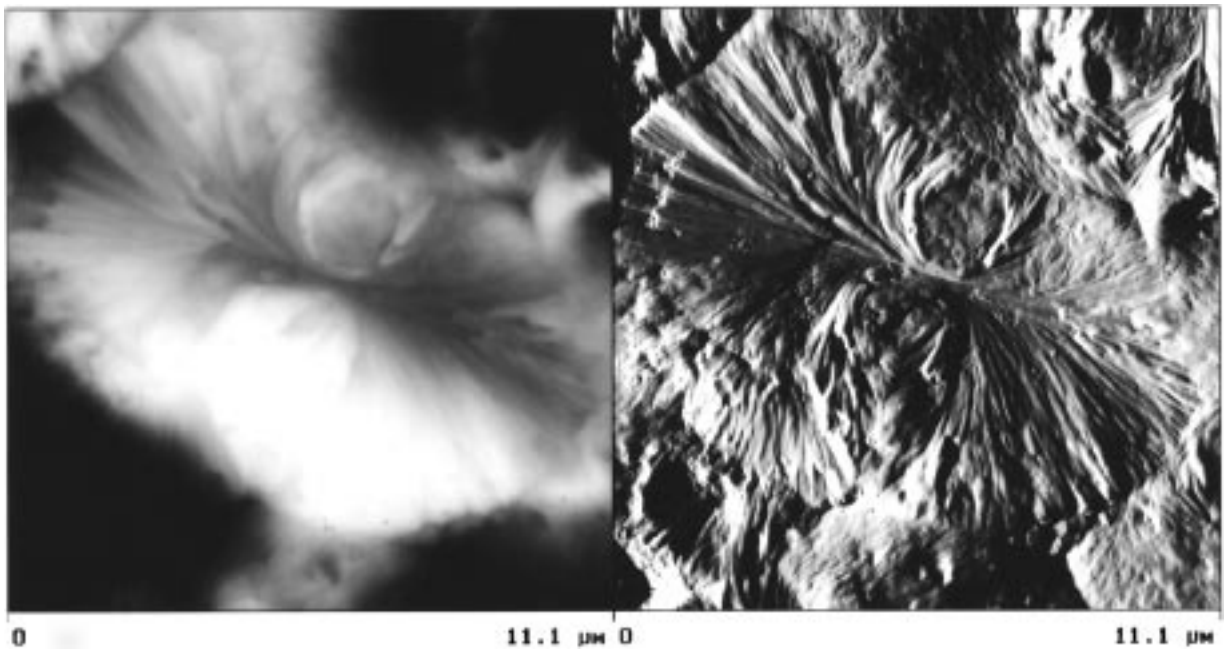

Figure 6. AFM images of PFS-100 crystallized at 100 °C: left image, height mode; right image, deflection mode. Scan size: 11 μm.

originates from the method of sample preparation. Melt crystallized samples show two sharp distinct reflections, whereas solution crystallized or film cast samples show only one broad peak. So far, no crystal structure has been indexed for poly(ferrocenyldimethylsilane).

In Figure 6, AFM images of a hedritic structure (height and deflection) are shown for PFS-100 after crystallization at 100 °C. Such hedritic structures consist of edge-on lamellae in the center of the morphological unit. This is displayed in the image which shows lamellae splaying with increasing radius, which curve and eventually close. In more matured stages of the crystallization, well-known spherulitic morphologies eventually form.[35] Similar hedritic structures were considered as nonmature stages of spherulitic growth for isotactic polystyrene[36] and isotactic polypropylene.[37]

AFM was also used to visualize the appearance of the basic morphological features prior to and after the peak I transition. To accomplish this, PFS-100 was isothermally crystallized at 90 °C, then cooled to room temperature, and imaged by AFM. Also, PFS-100 was crystallized at 90 °C and heated to 135 °C (which is beyond peak I and below peak II) and then cooled to room temperature for AFM study. Both samples displayed the same basic morphological features.

In this AFM study no quantitative evaluation of changes in the lamellar thickness or the long period was attempted. Instead, this was performed by quantitative SAXS analysis.

Figure 7 shows the long-period L of PFS-25 as a function of temperature after isothermal crystallization at 90 °C, deduced from the maximum of the SAXS intensity peak using Bragg's law. In Figure 7 the temperatures of transitions I and II, respectively, as determined on the DSC thermogram (see Figure 2a), are shown. The long-period increases from about 13 to 15.5 nm in the temperature range of our experiments.

The observed increase in the long-period (SAXS), in association with findings from DSC, WAXS, and AFM suggest that it is a lamellar thickness transformation which accounts for the multiple endotherms observed

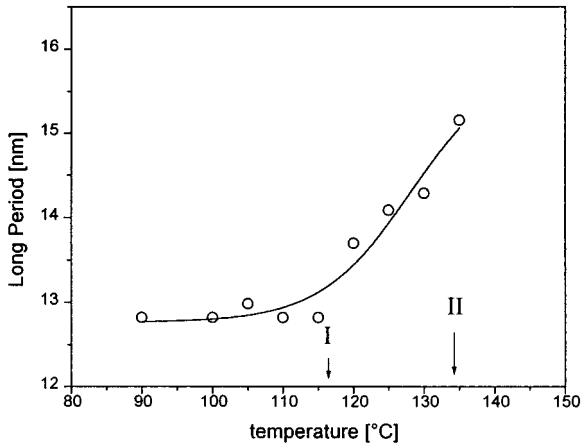

Figure 7. Long-period as a function of temperature for PFS-25 after isothermal crystallization at 90 °C.

in the DSC experiments. This is due to thin lamellae formed at high degrees of supercooling resulting in the first melting endotherm (type I) upon heating. Subsequently, recrystallization occurs when these thin lamellae melt. Since a large number of nuclei are still present up to the equilibrium melting temperature, the recrystallization occurs very rapidly, leading to thicker lamellae. These thicker lamellae melt at a higher temperature resulting in the second endotherm (type II).

Conclusions

The melting and crystallization behavior of a series of anionically prepared poly(ferrocenyldimethylsilanes) is described. The multiple melting endotherms observed in DSC experiments were ascribed to a reorganization process which occurs during the heating scan. The observed melting temperatures of crystals formed during isothermal crystallization could be described by the Hoffman−Weeks equation. The equilibrium melting temperature of poly(ferrocenyldimethylsilane) at 143 °C was obtained by extrapolation. AFM scans showed no morphological changes upon going through the multiple

endotherms. Wide-angle X-ray scattering experiments displayed no shifts of the crystalline reflections upon heating the sample up to the melt. Therefore, the reorganization process cannot be ascribed to polymorphism. During small-angle X-ray scattering experiments there was an increase observed in the long period upon heating through the type I endotherm. From these findings it was concluded that thinner lamellae, which are formed during isothermal crystallization, melt upon heating (peak I) and recrystallize into thicker lamellae. The thicker lamellae then melt at a higher temperature, giving rise to a second endotherm (peak II).

Acknowledgment. Financial support from the University of Twente is gratefully acknowledged. The authors would like to thank Dr. D. Trifonova (University of Twente) for the AFM imaging, the group of Prof. G. Strobl (University of Freiburg) and Dr. C.R. Jaeger (University of Twente) for their help with the SAXS and WAXS measurements, Ms. Fazila Seker (University of Toronto) for preliminary morphology studies, and Mr. L. O'Connor for editing the manuscript.

References and Notes

(1) (a) Manners, I. *J. Inorg. Organomet. Polym.* **1993**, *3*, 185. (b) Manners, I. *Adv. Organomet. Chem.* **1995**, *37*, 131.
(2) Hmyene, M.; Yassar, A.; Escotne, M.; Percheron-Guegan, A.; Garnier, F. *Adv. Mater.* **1994**, *6*, 564.
(3) Rosenberg, H. U.S. Pat. 3,426,053, 1969.
(4) Foucher, D. A.; Tang, B. Z.; Manners, I. *J. Am. Chem. Soc.* **1992**, *114*, 6246.
(5) Rasburn, J.; Petersen, R.; Jahr, T.; Rulkens, R.; Manners, I.; Vancso, G. J. *Chem. Mater.* **1995**, *7*, 871.
(6) (a) Ni, Y.; Rulkens, R.; Pudelski, J. K.; Manners, I. *Macromol. Rapid Commun.* **1995**, *16*, 637. (b) Gómez-Elipe, P.; Macdonald, P. M.; Manners, I. *Angew. Chem., Int. Ed. Engl.* **1997**, *36*, 762.
(7) (a) Rulkens, R.; Ni, Y.; Manners, I. *J. Am. Chem. Soc.* **1994**, *116*, 12121. (b) Rulkens, R.; Lough, A. J.; Manners, I. *J. Am. Chem. Soc.* **1994**, *116*, 797.
(8) Nguyen, M. T.; Diaz, A. F.; Dement'ev, V.; Pannell, K. H. *Chem. Mater.* **1993**, *5*, 1389.
(9) (a) Foucher, D. A.; Ziembinski, R.; Tang, B. Z.; Macdonald, P. M.; Massey, J.; Jaeger, C. R.; Vancso, G. J.; Manners, I. *Macromolecules* **1993**, *26*, 2878. (b) Pudelski, J. K.; Rulkens, R.; Foucher, D. A.; Lough, A. J.; Macdonald, P. M.; Manners, I. *Macromolecules* **1995**, *28*, 7301.
(10) (a) Nelson, J. M.; Rengel, H.; Manners, I. *J. Am. Chem. Soc.* **1993**, *115*, 7035. (b) Pudelski, J. K.; Gates, D. P.; Rulkens, R.; Lough, A. J.; Manners, I. *Angew. Chem., Int. Ed. Engl.* **1995**, *34*, 1506. (c) Angelakos, C.; Zamble, D. B.; Foucher, D. A.; Lough, A. J.; Manners, I. *Inorg. Chem.* **1994**, *33*, 1709. (d) Foucher, D. A.; Edwards, M.; Burrow, R. A.; Lough, A. J.; Manners, I. *Organometallics* **1994**, *13*, 3, 4959.
(11) Nelson, J. M.; Lough, A. J.; Manners, I. *Angew. Chem., Int. Ed. Engl.* **1994**, *33*, 989.
(12) Foucher, D.; Ziembinski, R.; Petersen, R.; Pudelski, J.; Edwards, M.; Ni, Y.; Massey, J.; Jaeger, C. R.; Vancso, G. J.; Manners, I. *Macromolecules* **1994**, *27*, 3992.
(13) Foucher, D. A.; Honeyman, C. H.; Nelson, J. M.; Tang, B. Z.; Manners, I. *Angew. Chem., Int. Ed. Engl.* **1993**, *32*, 1709.
(14) Tang, B. Z.; Petersen, R.; Foucher, D. A.; Lough, A.; Coombs, N.; Sodhi, R.; Manners, I. *J. Chem. Soc., Chem. Commun.* **1993**, 523.
(15) Ni, Y.; Rulkens, R.; Manners, I. *J. Am. Chem. Soc.* **1996**, *118*, 4102.
(16) Fischer, A. B.; Kinney, J. B.; Staley, R. H.; Wrighton, M. S. *J. Am. Chem. Soc.* **1979**, *101*, 6501.
(17) See, e.g.: Campbell, D.; White, J. R. *Polymer characterization*, Chapman and Hall: London, 1989; p 12.
(18) Fox, T. G.; Flory, P. J. *J. Appl. Phys.* **1950**, *21*, 581.
(19) O'Driscoll, K.; Amin Sanayei, R. *Macromolecules* **1991**, *24*, 4479.
(20) Cebe, P.; Hong, S. D. *Polymer* **1986**, *27*, 1183.
(21) Bassett, D. C.; Olley, R. H.; Al Raheil, I. A. M. *Polymer* **1988**, *29*, 1745.
(22) Blundell, D. J. *Polymer* **1987**, *28*, 2248.
(23) Cheng, S. Z. D.; Cao, M. Y.; Wunderlich, B. *Macromolecules* **1986**, *19*, 1868.
(24) Velikov, V.; Marand, H. *Bull. Am. Phys. Soc.* **1994**, *39*, 569.
(25) Holdsworth, P. J.; Turner-Jones, A. *Polymer* **1971**, *12*, 195.
(26) Alfonso, G. C.; Pedemonte, E.; Ponzetti, L. *Polymer* **1979**, *20*, 104.
(27) Lee, Y.; Porter, R. S. *Macromolecules* **1987**, *20*, 1336.
(28) Hsiao, B. S.; Gardner, K. H.; Wu, D. Q.; Chu, B. *Polymer* **1993**, *34*, 3996.
(29) Jonas, A. M.; Russell, T. P.; Yoon, D. Y. *Macromolecules* **1995**, *28*, 8491.
(30) Medellin-Rodriguez, F. J.; Philips, P. J.; Lin, J. S. *Macromolecules* **1996**, *29*, 7491.
(31) Pope, D. P. *J. Polym. Sci., Polym. Phys. Ed.* **1976**, *14*, 811.
(32) Lee, Y.; Porter, R. S.; Lin, J. S. *Macromolecules* **1989**, *22*, 1756.
(33) Hoffman, J. D.; Weeks, J. J. *J. Res. Natl. Bur. Stand.* (*U.S.*) **1962**, *66A*, 13.
(34) Rulkens, R.; Lough, A. J.; Manners, I.; Lovelace, S. R.; Grant, C.; Geiger, W. E. *J. Am. Chem. Soc.* **1996**, *118*, 12683.
(35) Bassett, D. C. *Philos. Trans. R. Soc. London.* **1994**, *348 A*, 29.
(36) Bassett, D. C.; Vaughan, A. S. *Polymer* **1985**, *26*, 717.
(37) Trifonova, D.; Varga, J.; Ehrenstein, G. W.; Vancso, G. J. *Polym. Prepr.* (*Am. Chem. Soc., Div. Polym. Chem.*) **1996**, *37* (2), 563; Submitted to *J. Polym. Sci., Polym. Phys. Ed.*

MA9711248